Electronic Supplementary Information

Manuscript title: Effect of Anodization Time on Photovoltaic Properties of Nanoporous Silicon based Solar Cells

Authors: Hamid Ghorbani Shiraz †

School of Chemical Engineering, College of Engineering, University of Tehran, Iran
Young Researchers and Elite Club, Mashhad Branch, Islamic Azad University, Mashhad, Iran

† E-mail: Ghorbani_Shiraz@ut.ac.ir
Tel.: +98 936 802 1420

S1

Structural component of image was delineated in Fig. 1 (a), was examined by Energy Dispersive Spectroscopy (EDS) analysis.

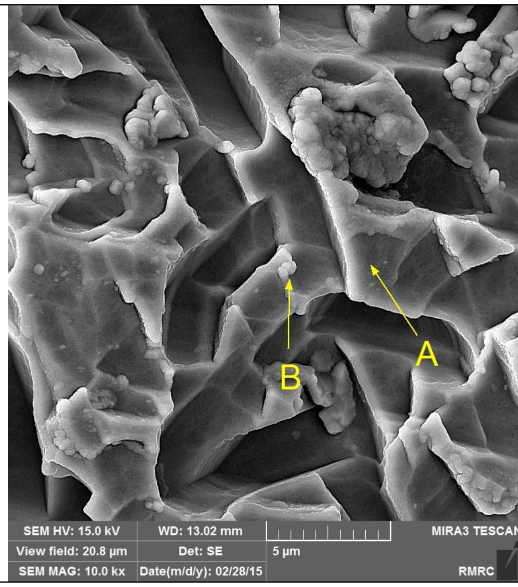

A

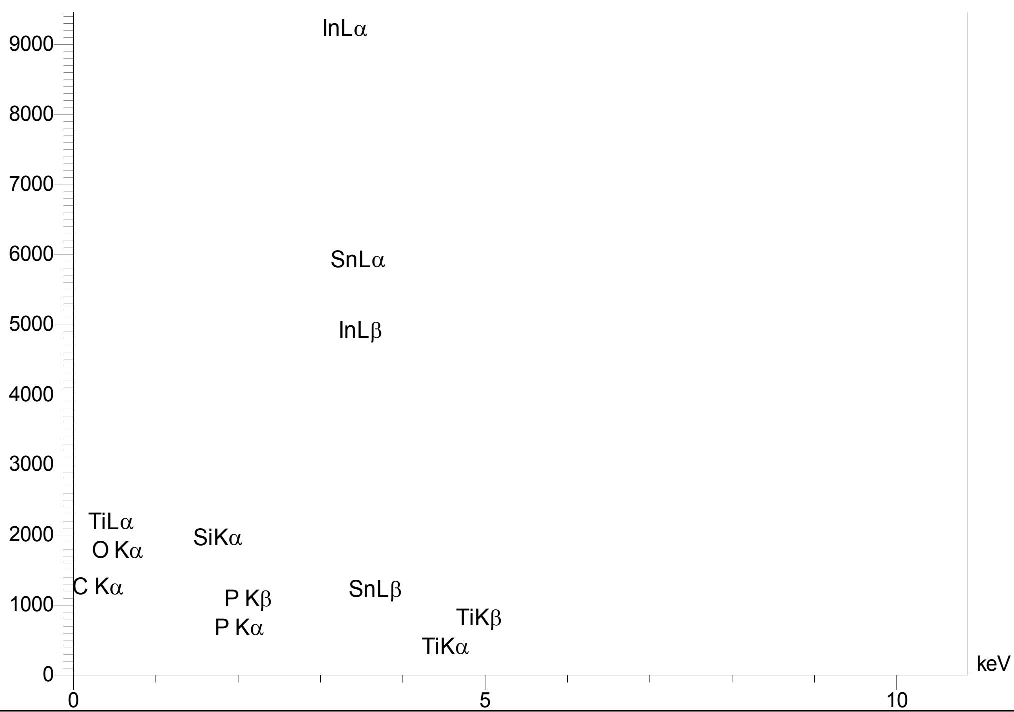

B

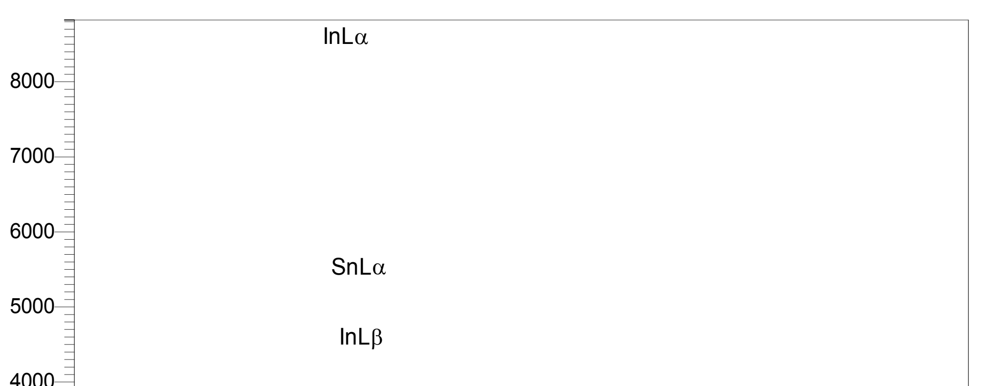

S2

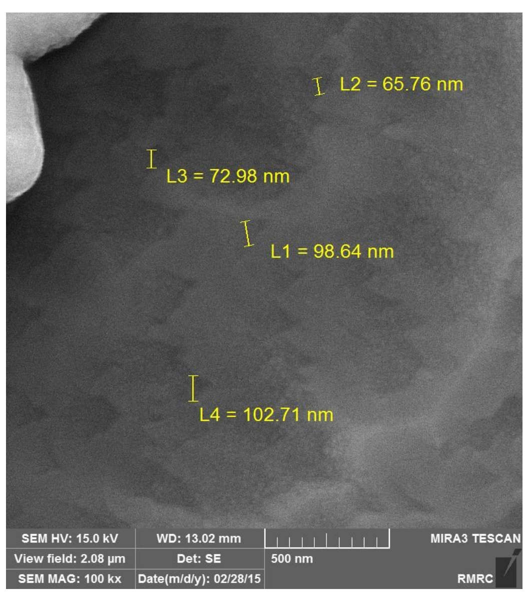
L2 = 65.76 nm
L3 = 72.98 nm
L1 = 98.64 nm
L4 = 102.71 nm
SEM HV: 15.0 kV
WD: 13.02 mm
MIRA3 TESCAN
View field: 2.08 μm
Det: SE
500 nm
SEM MAG: 100 kx
Date(m/d/y): 02/28/15
RMRC

Fig. S2. FESEM image of the Pores floor demonstrates even surface, hence the charge density could not satisfy for EPD

S3

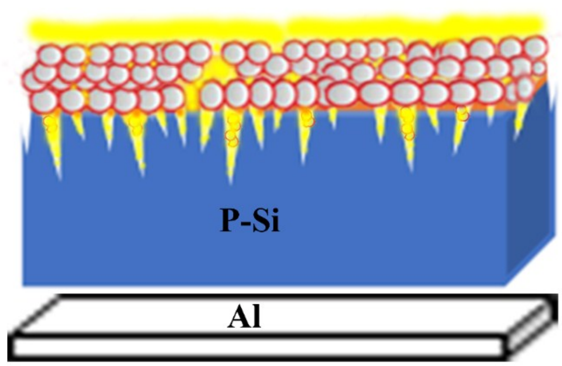

Fig. S3. Hybrid solar cell; n-type semiconductor (brown) has been kept just in the base of pores sidewall; porous structure has provided desirable substrate for TiO_2 nanoparticles (circle) immobilization also channels to p-type silicon; ITO (yellow) may diffuse through the channels; local p-n heterojunction have formed through minor diffusion of TiO_2 nanoparticles to the p-type pores.

Fig. S3 explains hierarchical steps to fabricate the proposed hybrid solar cell. Our target could be summarized as facilitating in p-n junction fabrication as well as making a hybrid model of silicon-nanostructure solar cells.

S4

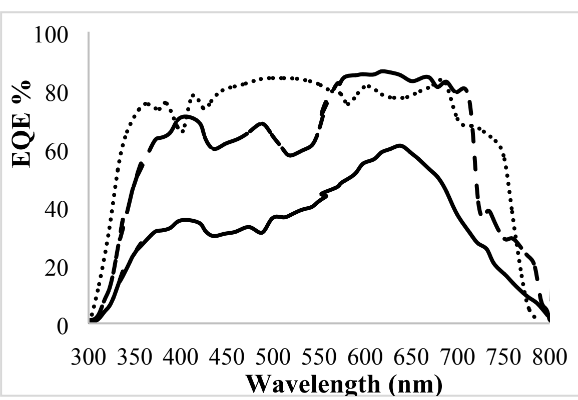

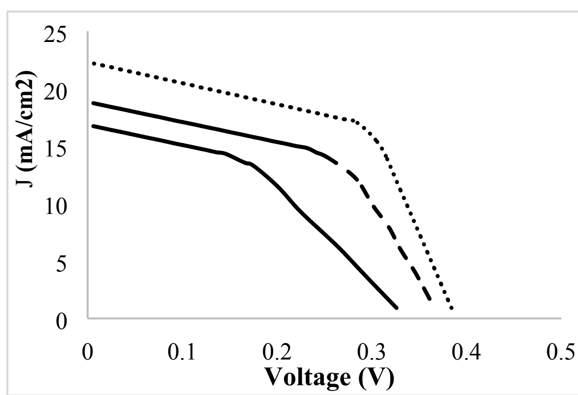

Fig. S4. Current density-Voltage (right) and External quantum efficiency (EQE) for samples; AD-6 (line), AD-8 (dash), and AD-10 (dot)

Fig. S4 (right) demonstrates the current density-voltage measurements for three competitive samples, AD-6, AD-8, and AD-10. Let's discuss about the resistances which could be received from J-V curves.
The shunt resistance is ascribed to the solar cell structural defects, rather than poor design. In fact, the limited shunt resistance allows the photocurrent to flow through alternate pathway. The alternative current path decreases the amount of current moving within junction and drops the voltage. A low light level could dramatically decrease the photocurrent; consequently, enhance the shunt resistance. As illustrated, all samples possess a relatively limited shunt resistance. It seems that the value of shunt resistance (reciprocal of slope at the J_{SC}) is equal for all samples. This demonstrated that the photocurrent paths, consequently the mechanism, are similar for all examined samples.
The series resistance could be translated from Fig. S4 (right), as the reciprocal of slope at the V_{OC}. In fact, the series resistance comes from recombination [21], especially recombination over defects and interfaces. In this regard, the series resistance could be attributed to the porous substrate; i.e. the distributed defects and tips could play as hot recombination centers. Since defects and tips possess low surface area, the charge density is very high in these regions [12]. Consequently, these regions are defined as the most capable location for recombination. Apart from that, dangling band plays a key role in recombination process [21]. That is why the high values obtained for (porous-based) samples. As illustrated in Fig. S4 (right), as the anodization time increases, the series resistance increases. This means that the porosity pattern is a decisive factor for distribution of recombination centers (defects and dangling band). As mentioned earlier in our previous study [12], the etching process could be conducted in both planar and level. Therefore, high anodization time could create several defects and/or dangling band; consequently, numerous recombination centers could be defined.
On the other hand, high anodization time could create depth pores. It is more likely that the high number of TiO_2 NPs immobilize into the pores. Therefore, several interface (recombination center) are defined between TiO_2 NPs and PS sidewalls.
Consequently, it is expected that the series resistance be in the order of AD-6 <AD-8 <AD-10. This order is in consistent with measurements which have been illustrated in Fig. S4 (right).
Following, the voltage loss is considered. The V_{OC} is the voltage characterizes when the forward bias diffusion current (I_{FB}) is equal to the J_{SC}. The I_{FB} directly correlates to the amount of recombination occurred within junction. Therefore, high amount of recombination enhances the I_{FB}, which in turn decreases the V_{OC}. Overall; there are decisive factors that effect on the V_{OC}: doping concentration, diffusion length, and defects. However, in the case of proposed architecture, the later factor comes more important compared to others. In fact, a high recombination centers within the diffusion length (defects, dangling bonds, and grain boundaries) disturb the charge transfer process through change in carrier pathways and recombination process. This phenomenon leads to significant reduction in V_{OC}.
As mentioned, the recombination centers distributed within samples (especially at junction) in the order of AD-6 < AD-8 < AD-10. Since these regions are capable for recombination, the recombination could be occurred in the same order. Consequently, the voltage loss could be evaluated significant in the case of AD-10.
Fig. S4 (left) shows the external quantum efficiency (EQE) spectrum of the examined samples. The J_{SC} calculated through integrating the EQE spectrum comes in consistent with the value obtained from J-V curve.

S5

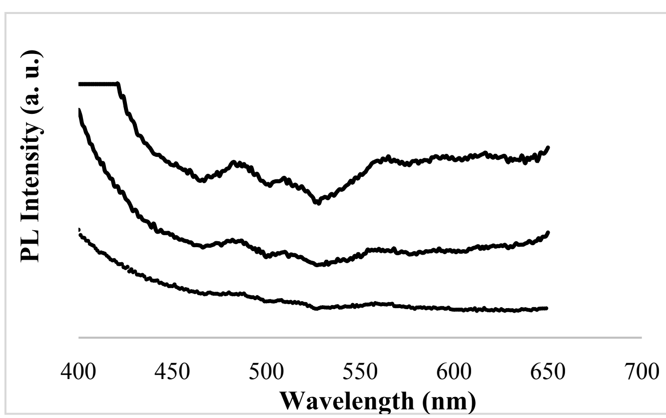

Fig. S5. PL characterizations for AD-6 (dot), AD-8 (dash), and AD-10 (line)